Ex-vivo Electrochemical pH Mapping of the Gastrointestinal Tract in the Absence and Presence of Pharmacological Agents

Teena S. Rajan,[1,2] Tania L. Read,[1] Aya Abdalla,[3] Bhavik A. Patel,[3] Julie V. Macpherson[1,*]

[1] *Department of Chemistry, University of Warwick, Gibbet Hill Road, CV4 7AL, UK*

[2]*Diamond Science and Technology CDT, University of Warwick, Coventry, CV4 7AL, UK*

[3]*School of Pharmacy and Biomolecular Science, University of Brighton, Brighton, BN2 4AT, UK*

** Corresponding Author*

Abstract: *Ex-vivo* pH profiling of the upper gastrointestinal (GI) tract (of a mouse), using an electrochemical pH probe, in both the absence and presence of pharmacological agents aimed at altering acid/bicarbonate production, is reported. Three pH electrodes were first assessed for suitability using a GI tract biological mimic buffer solution containing 0.5 % mucin. These include a traditional glass pH probe, an iridium oxide (IrOx) coated electrode (both operated potentiometrically) and a quinone (Q) surface-integrated boron doped diamond (BDD-Q) electrode (voltammetric). In mucin the timescale for both IrOx and glass to obtain stable pH readings was in the ~100's of s, most likely due to mucin adsorption, in contrast to 6 s with the BDD-Q electrode. Both the glass and IrOx pH electrodes were also compromised on robustness due to fragility and delamination (IrOx); contact with the GI tissue was an experimental requirement. BDD-Q was deemed the most appropriate. Ten measurements were made along the GI tract, esophagus (1), stomach (5) and duodenum (4). Under buffer only conditions, the BDD-Q probe tracked the pH from neutral in the esophagus, to acidic in the stomach and rising to more alkaline in the duodenum. In the presence of omeprazole, a proton pump inhibitor, the body regions of the stomach exhibited elevated pH levels. Under melatonin treatment (a bicarbonate agonist and acid inhibitor), both the body of the stomach and the duodenum showed elevated pH levels. This study demonstrates the versatility of the BDD-Q pH electrode for real-time *ex-vivo* biological tissue measurements.

Keywords: *Boron-doped diamond electrode, pH mapping, quinone voltammetry, gastrointestinal tract, ex-vivo, electrode fouling, mucin*

Disturbances in the pH homeostasis of the upper gastrointestinal (GI) tract, leads to many different health issues including gastritis, gastroduodenal ulceration, dyspepsia, and gastroesophageal reflux disease (GERD).[1–3] Under healthy conditions, the pH in the upper GI tract is maintained at ~7 in the esophagus, dropping to ~2 in the stomach and rising to pH 5-6 in the duodenum.[4–6] The low pH in the stomach is due to gastrin-stimulated proton-potassium pumps[7] in oxyntic glands secreting gastric acid.[8] Gastrin is secreted in response to chemical and mechanical stimulus.[9] In the duodenum, production and secretion of bicarbonate dominates, causing partial neutralization of acid entering from the stomach and resulting in a pH rise.[10] Alterations in gastric acid production and/or bicarbonate excess or deficiency result in disturbances to the pH homeostasis. Drugs such as omeprazole, treat excess acid production disorders such as GERD by reducing acid production in the stomach, due to their action as a proton pump inhibitor (PPI).[1,11] The hormone, melatonin, has been used effectively in combination with omeprazole for GERD treatment,[12] as it provides gastric mucosal protection by inhibiting acid secretion, whilst stimulating duodenal bicarbonate secretion.[13,14] Detecting pH changes across the GI can offer vital information to aid diagnosis and efficacy of treatments for GI related illnesses.

pH measurements are typically performed using potentiometric glass pH sensors.[15] These electrodes show a Nernstian (-59 mV/pH unit) response and high selectivity towards protons (H^+).[15,16] However, the glass membrane is fragile, the sensors can be bulky, the electrodes often require frequent recalibration due to potential drift, and a stable pH response can take minutes, dependent on solution conditions.[17] When miniaturization of the sensor is required, metal-metal oxide electrodes, in particular iridium oxide (IrOx) films are often used.[18–23] When electrochemically deposited, IrOx films exhibit Nernstian to super-Nernstian responses (-60 to -80 mV/pH unit).[21,24–26] Such electrodes have shown variability in response time ranging from 0.3 s to 190 s;[21,24,27–29] the longer response times are associated with increases in solution alkalinity.[21,24] High concentrations of chloride have been shown to result in film dissolution,[19] suggesting that IrOx films are not suitable for long-term application in chloride-containing systems.

Quinone (Q) functionalized carbon-based electrodes, operated as voltammetric pH sensors, have also attracted interest, as the quinones undergo proton coupled electron transfer ($Q + 2H^+ + 2e^- \rightarrow QH_2$) and thus show a Nernstian voltammetric pH response.[30] The quinones are either directly integrated into the electrode surface, as is the case for sp^2 bonded carbon materials[31–34] and hybrid sp^2-boron doped diamond electrodes (BDD-Q electrodes),[35] or are tethered chemically to the electrode surface.[36,37] The latter is far more susceptible to

degradation if the electrode requires mechanical cleaning. Q-functionalized electrodes perform well under buffered conditions, providing a pH response in the time taken to produce a voltammetric scan (i.e. seconds).[33–35] In unbuffered solutions, the situation is more complicated due to local proton depletion/accumulation during the voltammetric measurement. The use of low Q surface coverages coupled with pulsed voltammetric measurements[38] or Q structures that promote inter and intra-molecular hydrogen bonding,[39,40] have been explored to negate this effect.

There is limited information concerning pH measurements across the upper GI tract; measurements have largely focused on the stomach only, *ex-vivo* and *in-vivo*. For example, IrOx electrodes were used *ex-vivo* to measure the pH of isolated stomach tissue.[41,42] To minimize electrode fouling, measurements were made under flow, however, this comes at a loss of spatial resolution due to flow-induced mixing of local pH gradients. *In-vivo* pH measurements of gastric acid in the stomach were carried out using glass potentiometric electrodes,[43,44] whilst a BDD microelectrode placed in the stomach of a mouse was used to record stomach pH.[45] The latter measured the amperometric signal associated with proton reduction, however, unlike the techniques highlighted above, this method lacks selectivity for protons, any redox species active at the operating potential will be reduced. Although still in their infancy, *in-vivo* pH measurements have been performed using ingestible wireless transmitting capsules (*e.g.* SmartPill)[46] that record pH, pressure, and temperature during transit.[47,48] The pH component of the SmartPill is an ion-selective field effect transistor. Such devices suffer, however, from frequent loss of signal, large pH-drift, and difficulty in accurately determining the location of the capsule.[5]

In this paper we map the pH profile of the upper GI tract of a mouse, under first homeostasis and then in response to pharmacological treatment (both omeprazole and melatonin). The measurement is made under diffusion only conditions, to minimize flow induced pH mixing, and the electrode itself is used to mechanically stimulate the tissue in order to induce acid secretion. To determine the most suitable pH technology for this measurement, we first assess the suitability of three different electrochemical approaches, traditional pH sensitive glass, IrOx and BDD-Q in physiologically relevant 0.5 % *w/v* mucin. Mucin, which coats the surface of epithelial organs is a useful mimic for the GI environment,[49–51] and a common electrode fouling agent.[51] The most promising methodology, in terms of robustness, minimal fouling, ability to rapidly measure pH, with a spatial footprint capable of differentiating between different regions of the GI tract, is then applied.

Experimental

Solutions

Solutions were prepared using ultrapure water (Milli-Q, resistivity ≥ 18.2 MΩ cm at 25 °C). All chemicals were used as received. Carmody buffers were prepared over the physiological range pH 3-8 using boric acid (H_3BO_3, 99.97%, Sigma-Aldrich), citric acid monohydrate ($C_6H_8O_7$, ≥99.5%, Sigma-Aldrich), and tertiary sodium phosphate (Na_3PO_4, ≥95%, Sigma-Aldrich).[52] BDD/BDD-Q electrode characterizations were conducted in 0.1 M KNO_3 (99%, Sigma-Aldrich), 1 mM $(Ru(NH_3)_6^{3+/2+}$ (99%, Strem Chemicals), 0.1 M H_2SO_4 (Fisher Scientific), and pH 2 Carmody buffer. The IrOx deposition solution was prepared from iridium tetrachloride hydrate (99.9%, Alfa Aesar), hydrogen peroxide solution (H_2O_2, 30% w/w, Fisher Scientific), oxalic acid dihydrate (HO_2CCO_2H, ≥99%, Sigma Aldrich), and anhydrous potassium carbonate (K_2CO_3, ≥99%, Fisher Scientific). Mucin from porcine stomach (Sigma-Aldrich) 0.5 % *w/v* in HEPES buffer solution, pH 7.4 (135.5 mM NaCl, 5.9 KCl, 2.5 mM $CaCl_2$, 1.2 mM $MgSO_4$, 5.0 mM HEPES, 3.5 mM NaOH, 10.0 mM glucose) was prepared and used as a biological mimic of the GI tract environment. pH measurements were made using a Mettler Toledo SevenGo pH portable meter and InLab Expert Go-ISM glass probe (bulb size = 10 mm), kept in the Mettler Toledo InLab storage solution, when not in use. All pH electrodes were calibrated using Carmody buffers of pH 3, 4, 6, 7 and 8. Pharmacological tests were conducted on mouse GI tissue (2 months old, C57BL6) using 10 μM omeprazole ($C_{17}H_{19}N_3O_3S$, Sigma-Aldrich), and 1 μM melatonin ($C_{13}N_{16}N_2O_2$, ≥98%, Sigma-Aldrich) in HEPES buffer solution.

BDD and BDD-Q pH sensor fabrication and characterization

Polycrystalline BDD cylinders of 1 mm diameter (357 μm thickness; boron dopant density $>10^{20}$ B atoms cm^{-3}; minimal sp^2-carbon content, Element Six), polished on the top (growth) surface to approximately nanometer scale roughness, were machined from a 6 inch freestanding BDD wafer using a 355 nm Nd:YAG 34 ns laser micromachiner (E-355H-ATHI-O system, Oxford Lasers). The BDD cylinders were cleaned by immersing in ~200 °C, concentrated H_2SO_4 (analytical reagent grade ≥ 95 %, Fischer Scientific) saturated with KNO_3 for 30 mins. Samples were then rinsed with ultrapure water and cleaned in concentrated H_2SO_4 at ~200 °C for 30 minutes.[53] The BDD cylinders were annealed at 600 °C in air for 5 hours to remove any sp^2 bonded carbon created during the laser machining process.[53] To provide an Ohmic electric contact, Ti (10 nm) / Au (400 nm) was sputtered (Moorfields MiniLab 060 platform sputter/evaporator) onto the backside of the cylinder and

annealed at 400°C for 5 hours. These were then sealed in glass capillaries (O.D. 2 mm; I.D. 1.16 mm, Harvard Apparatus Ltd., Kent, U.K.) using the procedure outlined previously.[54]

For BDD-Q electrodes, the acid-cleaned and annealed BDD cylinders were laser micro-machined to produce a patterned hexagonal array of sixty-one sp^2-bonded carbon containing pits (diameter = 50±2 μm, depth = 5±2 μm, center-to-center spacing = 100 μm), following a published procedure.[35] Each pit was composed of a series of concentric rings, machined with a pulse fluence of ~14 J cm^{-2}, with pulses pitched at 1.5 μm, and rings pitched at 3 μm. After laser machining, the electrodes were acid cleaned at ~200 °C for 30 min in concentrated H_2SO_4 saturated with KNO_3, rinsed, followed by a final treatment in concentrated H_2SO_4 at ~200 °C for 30 minutes. This procedure leaves a very robust form of sp^2 bonded carbon, which has withstood the oxidative acid clean, in the laser machined regions of the BDD surface.[53] An Ohmic contact was formed and the BDD-Q sealed in glass, as described above. The electrode surface and pit profiles were analyzed *via* white light interferometry (WLI: Contour GT, Bruker).

Iridium oxide pH sensor fabrication and characterization

The IrOx solution was prepared as described in literature;[55,56] 4.45 mM iridium tetrachloride, 1 mL H_2O_2 (30 % w/w) and 39 mM oxalic acid dehydrate were added sequentially to 100 mL water and stirred for 30 min, 10 min, and 10 min intervals respectively. Anhydrous potassium carbonate was added until a pH of 10.5 was achieved resulting in a pale yellow-green solution. This was stirred for 48 h until the solution had stabilized and the appearance changed to a blue color. The IrOx solution was refrigerated between uses. Anodic electrodeposition of the film onto a BDD electrode (1 mm diameter) was performed in the IrOx deposition solution by holding the electrode at +0.8 V versus a saturated calomel electrode (SCE), from a starting potential of 0.0 V, for 65 s.[57] The pH response is reliant on the hydration of the film,[18,19] therefore, the resulting film was hydrated in pH 7 Carmody buffer for two days prior to use and stored in this buffer solution when not in use. After exposure to mucin, the electrode was polished and a fresh IrOx film redeposited for repeat measurements.

Electrochemical measurements

Electrochemical measurements (voltammetric or open circuit potential (OCP)) were conducted using a potentiostat (CHI-760E, CH Instruments Inc., USA, or AutoLab PGSTAT128N, Metrohm, UK). For the BDD-Q electrode, measurements were made using a SCE (IJ Cambria Scientific Ltd., UK), or a non-leak silver-silver chloride reference electrode

(Ag|AgCl, Alvatek Ltd., UK), and a platinum wire (Goodfellow) counter electrode. Prior to use the electrochemical response and quinone surface coverages associated with the laser micromachined sp^2 bonded carbon regions of the BDD-Q electrode were characterized using standard protocols described previously.[35,58] Given the very low Q surface coverages[38] and to negate any possible proton depletion/accumulation effects, the pH response of the BDD-Q electrode was recorded using square wave voltammetry (SWV) using previously defined parameters: frequency = 150 Hz, amplitude = 100 mV, step potential = 1 mV.[35,38] SWV also offers a reduced scan time over other pulse techniques such as differential pulse voltammetry. The BDD-Q electrode was stored dry when not in use. Between measurements, where necessary, the electrodes were polished first with alumina (0.05 μm, Buehler, Germany) paste on a microcloth pad (Buehler), and then on a wetted (ultrapure water) alumina-free pad.

For the glass pH probe, as commercial pH meters provide the user with only the final pH reading, to access the OCP-time data, the pH probe was connected to an AutoLab PGSTAT128N potentiostat. The OCP was measured (data point every 0.1 s) against a non-leak Ag|AgCl reference until the change in OCP was ≤ 0.1 mV (corresponding to 0.001 pH units respectively). Once stabilized the OCP was recorded for a further 30 s and the OCP data averaged over this time period, to give the final pH reading. The measurements were conducted in order of decreasing acidity. The glass pH electrode was stored in the Mettler Toledo InLab storage solution when not in use, and was cleaned in accordance with manufacturer guidelines by soaking the electrode in 0.1 M HCl solution.[59] For IrOx, OCP measurements were conducted against a non-leak Ag|AgCl reference, using the CHI-760E and the same protocol adopted for making stable OCP measurements. These measurements were conducted by first decreasing pH and then increasing, in repeat cycles, obtaining at least three measurements at each pH.

Field Emission Scanning Electron Microscopy

Field-emission scanning electron microscopy (FE-SEM) was used to image the BDD-Q electrode before and after SWV scans in 0.5% *w/v* mucin in HEPES buffer solution. FE-SEM was performed using a Zeiss Supra 55VP, using an in-lens detector at an acceleration voltage of 5 kV.

Biological preparation

Animal experiments were carried out in compliance with the relevant laws and institution (University of Brighton) guidelines. Experimental procedures were conducted under ARRIVE guidelines.[60] C57BL6 male mice (2 months old) were euthanized using CO_2

gas. The esophagus, stomach, and duodenum were isolated and placed in HEPES buffer solution (pH 7.4) prior to sample preparation. The tissue was then cut along the middle, lightly stretched, and pinned flat onto a polydimethylsiloxane (PDMS) plate using stainless steel pins (diameter = 50 μm), resulting in final tissue dimensions of ~ 1.5 × 5.5 cm. To keep the tissue viable, the pinned tissue was covered with HEPES buffer solution.

Biological experiments

For *ex-vivo* BDD-Q pH measurements, the tissue sample was positioned in the center of the PDMS plate, with the electrode mounted on a micromanipulator for reproducible placement on the tissue; counter and reference electrodes were positioned close-by (ES1, Figure S1). For each measurement, the BDD-Q electrode was brought into contact with the tissue (to mechanically stimulate acid production), and then retracted to ~ 0.5 mm using a micro-positioner to maintain a constant separation from the tissue; the tissue surface varied in height, especially in the mid-region of the stomach. After measurement, the electrode was removed, rinsed using ultrapure water, and returned to the tissue. One measurement was made on the esophagus, five on different regions of the stomach, and four on different regions of the duodenum. ESI 2, Figure S2, shows a schematic of the upper GI tract, outlining the areas where the measurements were made. The HEPES buffer was then replaced with omeprazole (10 μM)[61] in HEPES buffer, to assess the influence of the PPI. The tissue was then perfused using HEPES buffer and treated with the hormone melatonin (1 μM),[13] a stimulant for bicarbonate production in the duodenal mucosa, in HEPES buffer. Recordings commenced after 20 mins exposure to the specific treatment.

Data analysis

Data analysis was conducted using OriginPro 9.1 (OriginLab Corp.), Python 3.6 and GraphPad Prism 8. For BDD-Q the SWVs were smoothed using a rolling mean with a window of 10 data points, in order to remove low amplitude noise. The pH peak was identified using the first derivative method within the bounds +0.3 V to -0.2 V *vs* Ag|AgCl. Where the first derivative is equal to zero, a turning point occurs, and the peak minima are identified by a positive second derivative at that point. For each SWV, the peak current and potential values were recorded, and calibration curves were fitted using linear regression. To evaluate statistical differences in the pH of the tissue between treatments, a two-way ANOVA adjusted for Sidak correction was employed, an appropriate correction for multiple comparisons. Differences were considered statistically significant at a probability of $p < 0.05$.

Results and Discussion

Potentiometric pH sensing technologies

Figure 1 illustrates (i) the mode of action of the pH measurement and (ii) typical OCP-time traces in 0.5 % *w/v* mucin in HEPES buffer, for (a) glass and (b) IrOx pH electrodes. 0.5 % was deemed physiologically relevant based on measurement of mucin concentration extracted from the GI tract of a mouse, after placement of tissue in 25 mL of oxygenated Krebs buffer for a period of 1 hour. The glass and IrOx pH electrodes were calibrated by measuring the OCP in Carmody buffers (pH 3-8) before and after measurement in mucin. Between measurements the electrodes were gently rinsed with ultrapure water. For both electrodes, the calibrations pre- and post-placement in the mucin solution showed minimal difference in gradient and intercept (ESI 3, Figures S3 and S4). Using the pre-mucin placement calibration data, the OCPs were converted to pH values as shown in Figures 1aii and bii. Note, whilst for the same IrOx electrode, the calibration gradient is unaffected by placement in 0.5 % mucin, for each freshly prepared IrOx electrode, different calibration gradients were recorded (ESI 3, Figure S4). This could be due to the variation in Ir^{3+}/Ir^{4+} ratio, or the hydration level of the film.[19,62] The fact that the ratio or hydration level of the film cannot be precisely controlled means the electrode cannot be reproduced exactly each time.

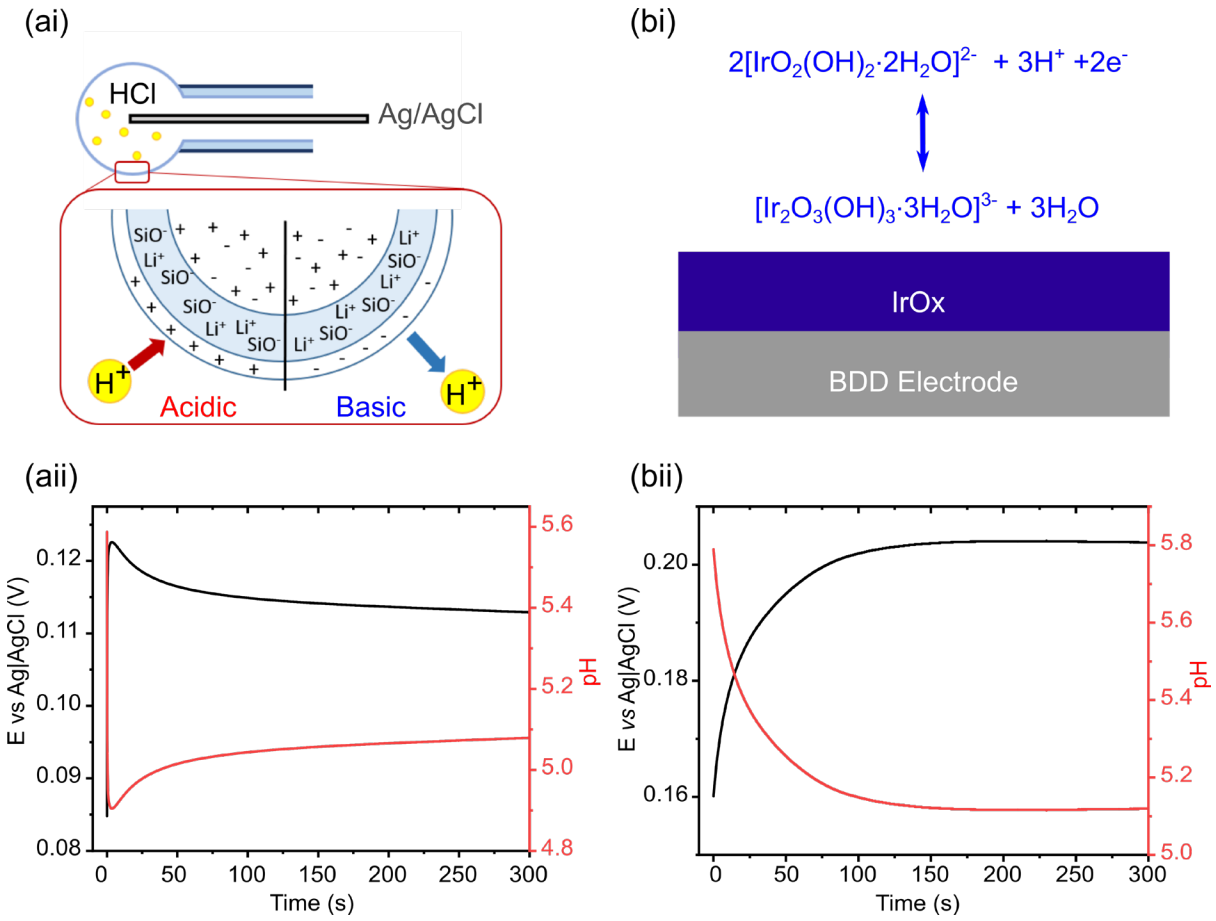

Figure 1. *Schematic of the potentiometric pH sensors (ai) glass pH electrode, and (bi) iridium oxide pH electrode (this electrode can operate potentiometrically or voltammmetrically, we use the potentiometric mode in this investigation). Open circuit potential measurements were conducted in 0.5 % w/v mucin in HEPES solutions using (aii) glass pH electrode, and (bii) iridium oxide pH electrode.*

OCP measurements in 0.5 % mucin HEPES solution were performed until the response ≤ 0.1 mV. From the data collected two pH values were determined one at ≤ 1 mV and the other ≤ 0.1 mV, which correspond to 0.01 and 0.001 pH units respectively, reflective of the stability criteria available on a commercial pH meter. This procedure was performed in triplicate for each electrode to demonstrate reproducibility. The average time required for the glass electrode to obtain a stable pH response in the mucin solution was 150 ± 60 s (≤ 1 mV) and 750 ± 60 s (≤ 0.1 mV), n = 3 (same electrode). For comparison, in mucin-free media (Carmody buffer pH 4) the response time was measured as 65 ± 17 s (≤ 1 mV) and 165 ± 60 s (≤ 0.1 mV), n = 3. Figure 1aii displays the first 300 s where the largest changes are evident. ESI 4, Figure S5, shows 800 s of OCP data collection for both electrodes. The pH of mucin measured with the glass pH probe, assuming ≤ 1 mV accuracy was 5.10 ± 0.04 (n =3) and 5.123 ± 0.013 (n=3) for ≤ 0.1 mV. A separate measurement in the same mucin solution using

the Mettler Toledo pH meter gave a pH of 5.020 ± 0.106 (automatic endpoint determination setting was set to 0.001 pH unit accuracy), $n = 3$ (same electrode and meter).

In Figure 1bii, the OCP-time profile is also shown for the IrOx electrode in 0.5 % *w/v* mucin HEPES solution, over 300 s. Here the electrode can be seen to reach a stable pH of 5.19 ± 0.08 (≤ 1 mV) and 5.200 ± 0.075 (≤ 0.1 mV) in 190 ± 35 s and 330 ± 104 s respectively, ($n = 3$, three different electrodes). In mucin-free media (Carmody buffer pH 4) the response time was measured as < 1 s (for both ≤ 1 mV and ≤ 0.1 mV). For the glass and IrOx electrodes the decreased times to reach a stable reading in the Carmody buffer suggests that mucin presence is significantly affecting stabilization times, possibly due to time-dependent adsorption effects.

The longer the stabilization time the less responsive the pH electrode is to dynamic pH changes. For both electrodes fairly lengthy stabilization timescales are required leading to greater diffusional mixing between local pH gradients on the GI tissue. Moreover, given the mouse GI tract dimensions, Figure S2, to map areas of interest, ten pH measurements every few mm along the length of the tract, are required. The size of the glass pH bulb diameter used (ca. 10 mm) poses a spatial problem for this application. Whilst it is possible to obtain pH-sensitive glass probes with smaller diameters (commercially 8-12 μm probes are available),[63] reduced size comes with significantly increased fragility. An essential part of this experiment is mechanical stimulation of the tissue, in the vicinity of the measurement, by the probe itself; the use of fragile micro-glass pH electrode would prove challenging. Contact of the probe with the tissue, for stimulation, is also problematic for the IrOx-coated electrode, which whilst of an appropriate size (1 mm diameter), is likely to suffer from the film being compromised upon mechanical impact with the tissue.

Voltammetric pH sensing technology

Figure 2a shows a WLI of a BDD-Q pH sensor, illustrating the position of the sixty-one laser-ablated pits in the BDD electrode surface. Figure 2b (inset) shows the first SWV scan at the BDD-Q electrode (0.6 to -0.3V, frequency: 150 Hz, amplitude: 0.1 V, increment: 1 mV) recorded in 0.5 % *w/v* mucin in HEPES solution. The time taken for one SWV scan is only 6 s and is an advantage of the voltammetric approach over both the OCP timescales for the glass and IrOx pH electrodes. Prior to measurement in mucin, the BDD-Q electrode was calibrated in pH 3-8 Carmody buffers ($n = 6$ per buffer). After recording the ten SWV scans (measurement time = 60 s), the BDD-Q electrode was gently rinsed and recalibrated. This

procedure was repeated using the same electrode and two other BDD-Q electrodes (i.e. $n = 4$ in total); calibrations shown in ESI 5, Figure S6. The pre- and post-calibrations, for each electrode, are very similar in gradient and intercept. The pre-mucin calibration was used to convert peak potential to pH. Figure 2b shows the pH values extracted from ten consecutive SWV scans in this media.

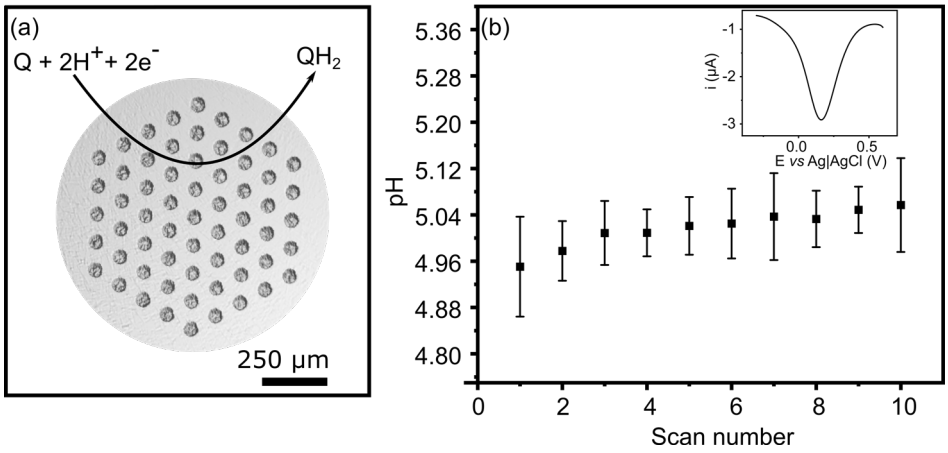

Figure 2. *(a) White light interferometry image of a BDD-Q pH electrode with the redox reaction responsible for the pH response, (b) average pH against scan number, for ten consecutive SWV scans conducted in 0.5% w/v mucin in HEPES solution, with standard deviation error bars n = 4; inset shows the first SWV scan for pH determination.*

FE-SEM images of the BDD-Q electrode surface after (a) polishing using alumina and rinsing with ultrapure water and (b) after ten consecutive SWV scans, removal from the 0.5 % mucin – HEPES solution and gentle rinsing of the electrode with water, are shown in Figure 3. In Figure 3a, the BDD grains (light and dark regions) are clearly visible, representing low and higher doped regions of the polished surface,[64] with three recessed laser-machined pits evident, which contain the sp^2 bonded carbon regions. After placement in mucin, running ten consecutive SWV scans and gently rinsing (Figure 3b), interestingly, whilst the image appears very similar, there is now little contrast, even though the imaging conditions were the same. This may suggest some mucin remaining on the surface even after the rinse process but is not conclusive. However, even if present, there is clearly not enough mucin to impact deleteriously on the calibration data, ESI 5.

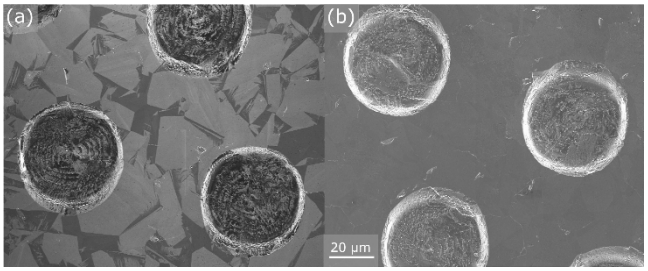

Figure 3. *FE-SEM images of BDD-Q pH electrode (a) polished with alumina slurry and rinsed, (b) after 10 consecutive SWV measurements in 0.5 % w/v mucin in HEPES buffer solution and rinsing.*

In the mucin-HEPES solution, taking the first scan data, Figure 2b, a pH value of 4.950 ± 0.086 was recorded. In comparison the Mettler Toledo pH meter recorded a value of 4.968 ± 0.131 (n = 4, same pH probe and meter). The error is slightly lower for the BDD-Q electrode than the glass pH probe. Considering the repeat scans, if errors are ignored and the average pH per scan number (black square data in Figure 2b) is compared, the data does show a very small decrease in peak potential (from 0.197 V to 0.190 V), equivalent to a pH increase from 4.951 to 5.057. The origin of this very small deviation in pH with repeat scans is under investigation. Mucin time-dependent adsorption[65] may be one possibility.

BDD-Q ex-vivo experiments

From an assessment of all three electrodes in terms of time required to record one pH value, the size and robustness of the electrode, and minimal shifts in the pre- and post-mucin calibrations, the BDD-Q electrode was deemed the most appropriate for GI tract pH mapping (Figure 4). Ten measurements were typically performed across the GI tissue sample, to include the esophagus (1), stomach (2-6) and duodenum (7-10).

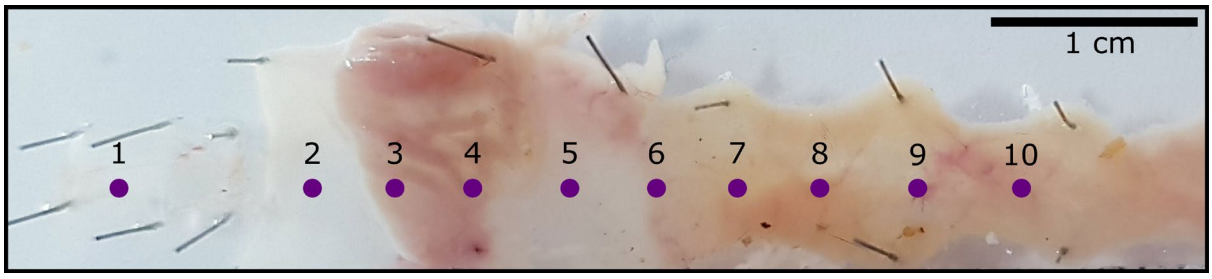

Figure 4. *Optical image of a mouse GI tract indicating the regions of pH measurement showing (1) esophagus, (2-6) stomach, and (7-10) duodenum.*

It was first necessary to validate that the pre-calibration of the BDD-Q electrode was not compromised by contact with the GI tract tissue. In order to assess the electrode

performance, nine measurements were performed across the GI tract (measurement 10 in Figure 4 was omitted due to tissue size), using three BDD-Q electrodes. Given the large variation in pH across the GI tract, whilst the very small change in pH arising from repetitive scans (Figure 2b) could be accommodated, a short rinse step (~ 10 s) was included between each measurement. This was a precaution to remove any possible mucin (or other species) adsorption exacerbated from contact with the tissue, during mechanical stimulation and was adopted in all GI tract measurements. Even with this rinse step the timescale for BDD-Q measurements is still faster than that possible with glass pH and IrOx electrodes based on the 0.5 % mucin data in Figures 1aii and 1bii. Importantly, calibration of the electrode pre- and post-tissue pH measurement showed minimal difference for all three BDD-Q electrodes (ESI 6, Figure S7) indicating the electrodes had not been compromised through contact with the tissue.

BDD-Q pH measurements across the mouse upper GI tract are shown in Figure 5, (a) in HEPES buffer only, (b) with the addition of 10 μM omeprazole and (c) with the addition of 1 μM melatonin, under stationary conditions. During these measurements the BDD-Q electrode was brought into contact with the tissue, to create the mechanical stimulus needed for acid secretion. Six tissues were used in total, i.e. n = 6, with the same BDD-Q electrode. The pH values recorded in Figure 5, represent the mean of these six samples, with the sample standard deviation as error bars. The pH was calculated using the buffer calibration recorded prior to each tissue measurement.

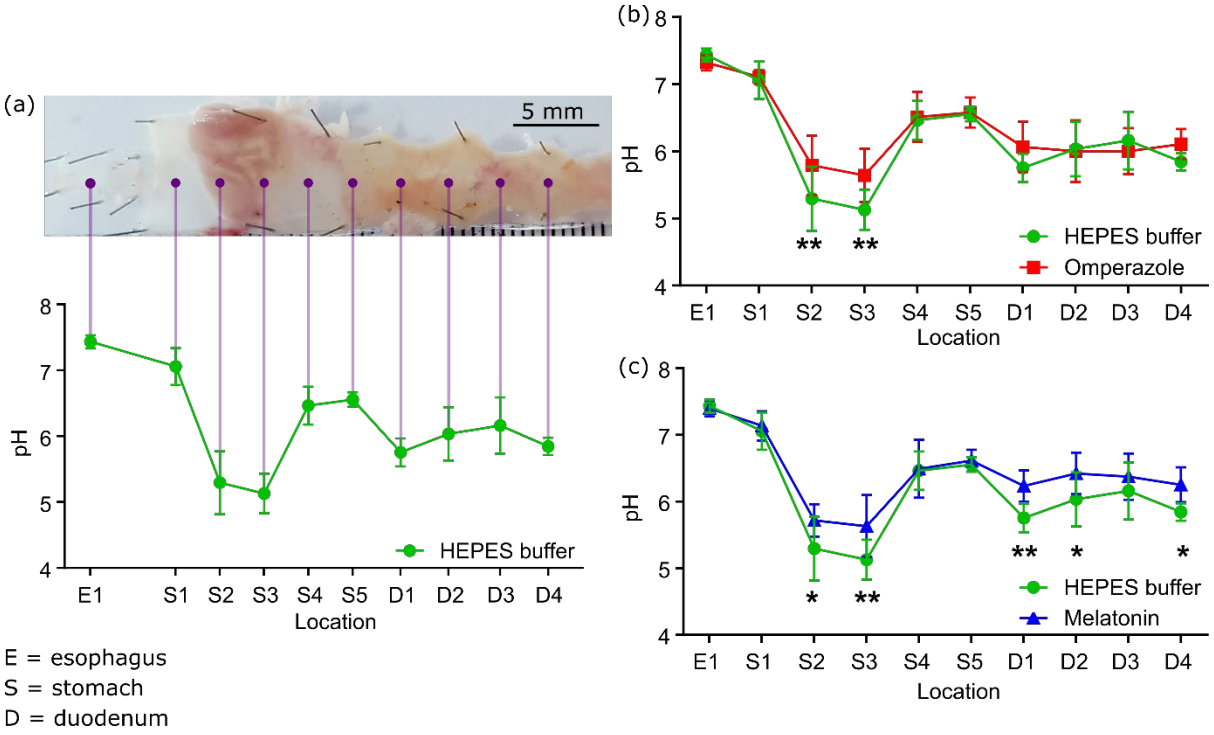

Figure 5. *BDD-Q electrode measurements of the pH across different regions of mouse gastrointestinal tract in (a) HEPES buffer solution only (green line), (b) 10 μM omeprazole in HEPES buffer solution (red line), and (c) 1 μM melatonin in HEPES buffer solution (blue line). Data represents an average of 6 tissue sample, with standard deviation error bars, where **p<0.01 and *p<0.05. Note the HEPES buffer measurement in (a-c) is the same data and was recorded prior to addition of either omeprazole or melatonin.*

In the absence of pharmacological treatments (Figure 5a), the esophagus is found to be neutral (E1 pH = 7.43 ± 0.097), while the stomach goes from neutral (S1 pH = 7.06 ± 0.28) to slightly acidic (S2 pH = 5.29 ± 0.48; S3 pH = 5.13 ± 0.30), before becoming more alkaline (S4 pH = 6.46 ± 0.29; S5 pH = 6.56 ± 0.11) towards the duodenum, which itself is more alkaline (D1 pH = 5.75 ± 0.21; D2 pH = 6.03 ± 0.41; D3 pH = 6.16 ± 0.43; D4 pH = 5.85 ± 0.13). The stomach pH is slightly higher than expected, but this is due to the acid secreted from the cells being buffered by the HEPES solution (pK_a = 7.56). These results demonstrate the effectiveness of the BDD-Q electrode at recording GI tissue pH. Conducting these measurements under static conditions and in close proximity to the tissue, allows for accurate spatial pH measurement in multiple locations along the upper GI tract.

Having successfully recorded pH measurements in physiologically typical tissue, the effects of pharmacological treatments were explored. Figure 5b shows the effect of adding omeprazole (10 μM) to the HEPES buffer solution. Here, a two-way ANOVA at a 5% significance level, with the Sidak correction for multiple comparisons was employed. The data demonstrates statistical significance in the pH of the body region of the stomach (S2 and S3), where the pH has risen, S2 pH = 5.79 ± 0.48; S3 pH = 5.64 ± 0.30, compared to that in untreated tissue. The tissue was then rinsed and left for 20 mins in HEPES buffer solution in order to help the tissue recover its original state. The buffer was then replaced with fresh solution containing 1 μM of melatonin in order to study the effect of this hormone on tissue pH. The pH response after melatonin treatment is presented in Figure 5c. Statistically significant differences in pH were observed in the duodenum and stomach (two-way ANOVA with Sidak correction). The D1-D4 regions of the duodenum and the body regions of the stomach (S2 and S3) all became more alkaline *i.e.* (D1 pH = 5.99 ± 0.25; D2 pH = 6.23 ± 0.35; D3 pH = 6.30 ± 0.37; D4 pH = 6.05 ± 0.36) and (S2 pH = 5.72 ± 0.24; S3 pH = 5.63 ± 0.46) compared to pH measurements in the untreated tissue.

Omeprazole is a known PPI targeting the H^+/K^+-ATPase pump in the body regions of the stomach. The pH mapping measurements clearly highlight the *ex-vivo* action of omeprazole in suppressing gastric acid release in the body regions of the stomach (S2 and S3)

of the GI tract, whilst leaving the esophagus and duodenum unaffected. Upon addition of melatonin, a potent bicarbonate agonist,[13,14] the pH probe demonstrates a statistically significant increase in pH in the duodenum regions of the GI tract (specifically D1, D2 and D4). Melatonin is also thought to inhibit gastric acid production,[14] and the pH probe shows statistically higher pH, again in the body regions of the stomach compared to the untreated tissue. Whilst this response could be due to melatonin, however, as the pH values recorded are very similar to those determined in the presence of omeprazole, it is possible omeprazole was left behind, even after flushing the tissue with buffer post-treatment.

Conclusion

This study reports the first *ex-vivo* pH profile map of the upper GI tract (of a mouse) from esophagus to duodenum, in the absence and presence of the pharmacological agents, omeprazole and melatonin, using an electrochemical pH sensor. pH electrodes for measurement in this *ex-vivo* environment ideally require the following properties, (i) high temporal resolution (the longer the measurement timescale the greater the impact of diffusional mixing from neighboring zones); (ii) a meaningful spatial resolution, ≤ 1 mm for the tissue employed herein; (iii) robustness, as contact with the tissue was used to both mechanically stimulate acid release and maintain a constant height separation and (iv) minimal impact of biological adsorption. Of the three pH electrodes assessed, BDD-Q appeared the most promising, recording the fastest response time (6 s versus ~100's of s), having an appropriate spatial footprint, and suitable robustness for repeated contact with the tissue surface.

Using BDD-Q it was possible to track the pH falling from near neutral conditions in the esophagus, to acidic in the stomach and rising to more alkaline in the duodenum. The importance of spatial resolution was illustrated by employing a small enough BDD-Q probe such that clear pH variations could be visualized even within specific regions of the GI tract (stomach). Utilizing a robust, stable probe was also important in enabling the impact of pharmacological treatment protocols to be readily assessed on the same tissue using the same probe. Adding omeprazole caused the body regions of the stomach to rise in pH, whilst melatonin resulted in an increase in pH in both the body regions of the stomach and the duodenum. To combat any possible electrode fouling from tissue contact the probe was briefly rinsed in between measurement. Future work would look to *in-situ* cleaning routes. Given, one advantage of a voltammetric sensor (BDD-Q), over a potentiometric one (IrOx and glass) is the ability to apply currents/voltages, electrochemical *in-situ* cleaning routes

could be considered. Finally, possible future developments could also see this technology move from *ex-vivo* to *in-vivo* through incorporation of the BDD-Q sensor into endoscopic probes or ingestible wireless transmitting capsules.

Associated Content

Supporting Information

The Supporting Information is available free of charge:

ESI 1, electrochemical set-up for ex-vivo upper gastrointestinal tract pH measurements; ESI 2, diagram of the upper gastrointestinal tract; ESI 3, glass and IrOx pH electrode pre- and post-mucin calibrations; ESI 4, stabilization potential-time for glass and IrOx pH electrodes in 0.5 % w/v mucin solution; ESI 5, BDD-Q pH electrode pre- and post-mucin calibration; ESI 6, biological method validation calibrations (PDF).

Author Information

Corresponding Author

*Email: j.macpherson@warwick.ac.uk

ORCID

Teena S. Rajan: 0000-0002-7993-5751

Tania L. Read: 0000-0002-9256-174X

Aya Abdalla: 0000-0001-7814-1442

Bhavik Anil Patel: 0000-0002-8773-3850

Julie V. Macpherson: 0000-0002-4249-8383

Notes

The authors declare no competing financial interest.

Author Credit

TSR performed methodology, formal analysis, investigation, writing-original draft, writing – reviewing and editing, and visualization. TLR performed conceptualization, writing – review and editing, and visualization. AA performed investigation, supervision, and writing – review and editing. BAP supplied conceptualization, methodology, formal analysis, resources, writing – review and editing, supervision and visualization. JVM supplied conceptualization, resources, writing – reviewing and editing, supervision, project administration, and funding acquisition.

Acknowledgements

We acknowledge the Royal Society for an Industrial Fellowship (JVM INF/R1/180026) and the EPSRC Centre for Doctoral Training in Diamond Science and Technology (TSR EP/L015315/1). The authors acknowledge use of Electron Microscopy Research Technology Platform facilities at the University of Warwick, Miss Georgia Wood for assistance with FE-SEM, and Dr Gabriel Meloni and Prof. Patrick Unwin for helpful discussions.

References

(1) Hunt, R. H. Importance of pH Control in the Management of GERD. *Arch. Intern. Med.* **1999**, *159* (7), 649–657.

(2) Holzer, P. Acid Sensing in the Gastrointestinal Tract. *Am. J. Physiol. Gastrointest. Liver Physiol.* **2007**, *292* (3), G699-705.

(3) Ostlie, D. J.; Holcomb, G. W. Gastroesophageal Reflux. *Ashcraft's Pediatr. Surg.* **2010**, 379–390.

(4) Evans, D. F.; Pye, G.; Bramley, R.; Clark, A. G.; Dyson, J.; Hardcastle, J. D.; Dyson, T. J.; Hardcastle, J. D. Measurement of Gastrointestinal pH Profiles in Normal Ambulant Human Subjects. *Gut* **1988**, *29*, 1035–1041.

(5) Maurer, J. M.; Schellekens, R. C. A.; Van Rieke, H. M.; Wanke, C.; Iordanov, V.; Stellaard, F.; Wutzke, K. D.; Dijkstra, G.; Van Der Zee, M.; Woerdenbag, H. J.; Frijlink, H. W.; Kosterink, J. G. W. Gastrointestinal pH and Transit Time Profiling in Healthy Volunteers Using the IntelliCap System Confirms Ileo-Colonic Release of ColoPulse Tablets. *PLoS One* **2015**, *10* (7), 1–17.

(6) Koziolek, M.; Grimm, M.; Becker, D.; Iordanov, V.; Zou, H.; Shimizu, J.; Wanke, C.; Garbacz, G.; Weitschies, W. Investigation of pH and Temperature Profiles in the GI Tract of Fasted Human Subjects Using the Intellicap® System. *J. Pharm. Sci.* **2015**, *104* (9), 2855–2863.

(7) Spencer, G.; Metz, D. C. Gastric Acid Secretion and Hormones. In *Practical Gastroenterology and Hepatology: Esophagus and Stomach*; Talley, N. J., DeVault, K. R., Fleischer, D. E., Eds.; Wiley-Blackwell, 2010; pp 16–21.

(8) Joseph, I. M. P.; Zavros, Y.; Merchant, J. L.; Kirschner, D. A Model for Integrative Study of Human Gastric Acid Secretion. *J. Appl. Physiol.* **2003**, *94*, 1602–1618.

(9) Schubert, M. L.; Peura, D. A. Control of Gastric Acid Secretion in Health and Disease. *Gastroenterology* **2008**, *134* (7), 1842–1860.

(10) Widmaier, E. P.; Raff, H.; Strang, K. T. The Digestion and Absorption of Food. In *Vander's Human Physiology, The Mechanisms of Body Function*; McGraw-Hill Higher Education, 2008; pp 528–565.

(11) Lindberg, P.; Brndstrm, A.; Wallmark, B.; Mattsson, H.; Rikner, L.; Hoffmann, K. J. Omeprazole: The First Proton Pump Inhibitor. *Med. Res. Rev.* **1990**, *10* (1), 1–54.

(12) Kandil, T. S.; Mousa, A. A.; El-Gendy, A. A.; Abbas, A. M. The Potential Therapeutic Effect of Melatonin in Gastro-Esophageal Reflux Disease. *BMC Gastroenterol.* **2010**, *10* (7), 1–9.

(13) Sjöblom, M.; Flemström, G. Melatonin in the Duodenal Lumen Is a Potent Stimulant of Mucosal Bicarbonate Secretion. *J. Pineal Res.* **2003**, *34*, 288–293.

(14) Bang, C. S.; Yang, Y. J.; Baik, G. H. Melatonin for the Treatment of Gastroesophageal Reflux Disease; Protocol for a Systematic Review and Meta-Analysis. *Medicine (Baltimore).* **2019**, *98* (4), e14241.

(15) Skoog, D. A.; Holler, F. J.; Crouch, S. R. *Principles of Instrumental Analysis*, 7th Editio.; Cengage Learning: Boston, USA, 2016.

(16) Ghoneim, M. T.; Nguyen, A.; Dereje, N.; Huang, J.; Moore, G C; Murzynowski, P. J.; Dagdeviren, C. Recent Progress in Electrochemical pH-Sensing Materials and Configurations for Biomedical Applications. *Chem. Rev.* **2019**, *119*, 5248–5297.

(17) Kristensen, H. B.; Kokholm, G. International pH Scales and Certification of pH. *Anal. Chem.*

1991, *63* (18), 885–891.

(18) Głab, S.; Hulanicki, A.; Gunnar, E.; Ingman, F. Metal-Metal Oxide and Metal Oxide Electrodes as pH Sensors. *Crit. Rev. Anal. Chem.* **1989**, *21* (1), 29–47.

(19) O'hare, D.; Parker, K. H.; Winlove, C. P. Metal-Metal Oxide pH Sensors for Physiological Application. *Med. Eng. Phys.* **2006**, *28*, 982–988.

(20) Daomin Zhou, D. Microelectrodes for In-Vivo Determination of pH. In *Electrochemical Sensors, Biosensors and their Biomedical Application*; 2008; pp 261–305.

(21) Ng, S. R.; O'Hare, D. An Iridium Oxide Microelectrode for Monitoring Acute Local pH Changes of Endothelial Cells. *Analyst* **2015**, *140*, 4224–4231.

(22) Manjakkal, L.; Szwagierczak, D.; Dahiya, R. Metal Oxides Based Electrochemical pH Sensors: Current Progress and Future Perspectives. *Progess Mater. Sci.* **2020**, *109*, 100635.

(23) Patel, B. A.; Anastassiou, C. A.; O'Hare, D. Biosensor Design and Interfacing. In *Body Sensor Networks*; Yang, G.-Z., Ed.; Springer-Verlag London Limited, 2006; pp 41–88.

(24) Marzouk, S. A. M.; Ufer, S.; Buck, R. P.; Johnson, T. A.; Dunlap, L. A.; Cascio, W. E. Electrodeposited Iridium Oxide pH Electrode for Measurement of Extracellular Myocardial Acidosis during Acute Ischemia. *Anal. Chem.* **1998**, *70*, 5054–5061.

(25) Tolosa, V. M.; Wassum, K. M.; Maidment, N. T.; Monbouquette, H. G. Electrochemically Deposited Iridium Oxide Reference Electrode Integrated with an Electroenzymatic Glutamate Sensor on a Multi-Electrode Array Microprobe. *Biosens. Bioelectron.* **2013**, *42* (1), 256–260.

(26) Bezbaruah, A. N.; Zhang, T. C. Fabrication of Anodically Electrodeposited Iridium Oxide Film PH Microelectrodes for Microenvironmental Studies. *Anal. Chem.* **2002**, *74* (22), 5726–5733.

(27) Kinlen, P. J.; Heider, J. E.; Hubbard, D. E. A Solid-State pH Sensor Based on a Nafion-Coated Iridium Oxide Indicator Electrode and a Polymer-Based Silver Chloride Reference Electrode. *Sensors Actuators B* **1994**, *22*, 13–25.

(28) Huang, W.-D. D.; Cao, H.; Deb, S.; Chiao, M.; Chiao, J. C. A Flexible pH Sensor Based on the Iridium Oxide Sensing Film. *Sensors Actuators, A Phys.* **2011**, *169*, 1–11.

(29) da Silva, G. M.; Lemos, S. G.; Pocrifka, L. A.; Marreto, P. D.; Rosario, A. V.; Pereira, E. C. Development of Low-Cost Metal Oxide pH Electrodes Based on the Polymeric Precursor Method. *Anal. Chim. Acta* **2008**, *616* (1), 36–41.

(30) Kahlert, H. Functionalized Carbon Electrodes for pH Determination. *J. Solid State Electrochem.* **2008**, *12* (10), 1255–1266.

(31) Galdino, F. E.; Smith, J. P.; Kwamou, S. I.; Kampouris, D. K.; Iniesta, J.; Smith, G. C.; Bonacin, J. A.; Banks, C. E.; Flávia, F.; Galdino, E.; Smith, J. P.; Kwamou, S. I.; Kampouris, D. K.; Iniesta, J.; Smith, G. C.; Bonacin, J. A.; Banks, C. E. Graphite Screen-Printed Electrodes Applied for the Accurate and Reagentless Sensing of pH. *Anal. Chem.* **2015**, *87*, 11666–11672.

(32) Lafitte, V. G. H.; Wang, W.; Yashina, A. S.; Lawrence, N. S. Anthraquinone-Ferrocene Film Electrodes: Utility in pH and Oxygen Sensing. *Electrochem. commun.* **2008**, *10* (12), 1831–1834.

(33) Lu, M.; Compton, R. G. Voltammetric pH Sensing Using Carbon Electrodes: Glassy Carbon Behaves Similarly to EPPG. *Analyst* **2014**, *139*, 4599–4605.

(34) Lu, M.; Compton, R. G. Voltammetric pH Sensor Based on an Edge Plane Pyrolytic Graphite Electrode. *Analyst* **2014**, *139*, 2397–2403.

(35) Ayres, Z. J.; Borrill, A. J.; Newland, J. C.; Newton, M. E.; Macpherson, J. V. Controlled Sp 2 Functionalization of Boron Doped Diamond as a Route for the Fabrication of Robust and Nernstian pH Electrodes. *Anal. Chem.* **2016**, *88*, 974–980.

(36) Wildgoose, G. G.; Pandurangappa, M.; Lawrence, N. S.; Jiang, L.; Jones, T. G. J.; Compton, R. G. Anthraquinone-Derivatised Carbon Powder: Reagentless Voltammetric pH Electrodes. *Talanta* **2003**, *60*, 887–893.

(37) Lee, P. T.; Harfield, J. C.; Crossley, A.; Pilgrim, B. S.; Compton, R. G. Significant Changes in pKa between Bulk Aqueous Solution and Surface Immobilized Species: Ortho-Hydroquinones. *RSC Adv.* **2013**, *3*, 7347–7354.

(38) Cobb, S. J.; Ayres, Z. J.; Newton, M. E.; Macpherson, J. V. Deconvoluting Surface-Bound Quinone Proton Coupled Electron Transfer in Unbuffered Solutions: Toward a Universal Voltammetric pH Electrode. *JACS* **2019**, *141* (2), 1035–1044.

(39) Dai, C.; Song, P.; Wadhawan, J. D.; Fisher, A. C.; Lawrence, N. S. Screen Printed Alizarin-Based Carbon Electrodes: Monitoring pH in Unbuffered Media. *Electroanalysis* **2015**, *27* (4), 917–923.

(40) Dai, C.; Chan, C.-W. I.; Barrow, W.; Smith, A.; Song, P.; Potier, F.; Wadhawan, J. D.; Fisher, A. C.; Lawrence, N. S. A Route to Unbuffered pH Monitoring: A Novel Electrochemical Approach. *Electrochim. Acta* **2016**, *190*, 879–886.

(41) Bitziou, E.; O'Hare, D.; Patel, B. A. Simultaneous Detection of pH Changes and Histamine Release from Oxyntic Glands in Isolated Stomach. *Anal. Chem.* **2008**, *80* (22), 8733–8740.

(42) Bitziou, E.; Patel, B. A. Simultaneous Detection of Gastric Acid and Histamine Release to Unravel the Regulation of Acid Secretion from the Guinea Pig Stomach. *Am. J. Physiol. Liver Physiol.* **2012**, *303* (3), G396–G403.

(43) Synnerstad, I.; Johansson, M.; Nylander, O.; Holm, L. Intraluminal Acid and Gastric Mucosal Integrity: The Importance of Blood-Borne Bicarbonate. *Am. J. Physiol. - Gastrointest. Liver Physiol.* **2001**, *280*, G121–G129.

(44) Schade, C.; Flemström, G.; Holm, L. Hydrogen Ion Concentration in the Mucus Layer on Top of Acid-Stimulated and -Inhibited Rat Gastric Mucosa. *Gastroenterology* **1994**, *107* (1), 180–188.

(45) Fierro, S.; Seishima, R.; Nagano, O.; Saya, H.; Einaga, Y. In Vivo pH Monitoring Using Boron Doped Diamond Microelectrode and Silver Needles: Application to Stomach Disorder Diagnosis. *Sci. Rep.* **2013**, *3*, 3257.

(46) Kalantar-Zadeh, K.; Ha, N.; Ou, J. Z.; Berean, K. J. Ingestible Sensors. *ACS Sensors* **2017**, *2* (4), 468–483.

(47) Mikolajczyk, A. E.; Watson, S.; Surma, B. L.; Rubin, D. T. Assessment of Tandem Measurements of pH and Total Gut Transit Time in Healthy Volunteers. *Clin. Transl. Gastroenterol.* **2015**, *6*, 1–8.

(48) Beardslee, L.; Banis, G.; Chu, S.; Liu, S.; Chapin, A.; Stine, J.; Pasricha, P. J.; Ghodssi, R. Ingestible Sensors and Sensing Systems for Minimally Invasive Diagnosis and Monitoring: The Next Frontier in Minimally Invasive Screening. *ACS Sensors* **2020**, *5* (4), 891–910.

(49) Perez-Vilar, J.; Hill, R. L. The Structure and Assembly of Secreted Mucins. *J. Biol. Chem.* **1999**, *274* (45), 31751–31754.

(50) Corfield, A. P. Mucins: A Biologically Relevant Glycan Barrier in Mucosal Protection. *BBA - Gen. Subj.* **2015**, *1850*, 236–252.

(51) Fagan-Murphy, A.; Watt, F.; Morgan, K. A.; Patel, B. A. Influence of Different Biological

Environments on the Stability of Serotonin Detection on Carbon-Based Electrodes. *J. Electroanal. Chem.* **2012**, *684*, 1–5.

(52) Carmody, W. R. An Easily Prepared Wide Range Buffer Series. *J. Chem. Educ.* **1961**, *38* (11), 559–560.

(53) Cobb, S. J.; Laidlaw, F. H. J.; West, G.; Wood, G.; Newton, M. E.; Beanland, R.; Macpherson, J. V. Assessment of Acid and Thermal Oxidation Treatments for Removing Sp2 Bonded Carbon from the Surface of Boron Doped Diamond. *Carbon N. Y.* **2020**, *In Press*.

(54) Hutton, L.; Newton, M. E.; Unwin, P. R.; Macpherson, J. V. Amperometric Oxygen Sensor Based on a Platinum Nanoparticle-Modified Polycrystalline Boron Doped Diamond Disk Electrode. *Anal. Chem* **2009**, *81*, 1023–1032.

(55) Yamanaka, K. Anodically Electrodeposited Iridium Oxide Films. *Jpn. J. Appl. Phys.* **1989**, *28* (4), 632–637.

(56) Yamanaka, K. The Electrochemical Behavior of Anodically Electrodeposited Iridium Oxide Films and the Reliability of Transmittance Variable Cells. *Jpn. J. Appl. Phys.* **1991**, *30* (6), 1285–1289.

(57) Bitziou, E.; Joseph, M. B.; Read, T. L.; Palmer, N.; Mollart, T.; Newton, M. E.; Macpherson, J. V. In Situ Optimization of PH for Parts-Per-Billion Electrochemical Detection of Dissolved Hydrogen Sulfide Using Boron Doped Diamond Flow Electrodes. *Anal. Chem.* **2014**, *86*, 10834–10840.

(58) Ayres, Z. J.; Cobb, S. J.; Newton, M. E.; Macpherson, J. V. Quinone Electrochemistry for the Comparative Assessment of Sp 2 Surface Content of Boron Doped Diamond Electrodes. *Electrochem. commun.* **2016**, *72*, 59–63.

(59) Toledo, M. Seven2Go^{TM} pro PH/Ion Meter S8 Operating Instructions. 2014, p 44.

(60) Kilkenny, C.; Browne, W. J.; Cuthill, I. C.; Emerson, M.; Altman, D. G. Improving Bioscience Research Reporting: The Arrive Guidelines for Reporting Animal Research. *PLoS Biol.* **2010**, *8* (6), 1–5.

(61) Larsson, H.; Carlsson, E.; Junggren, U.; Olbe, L.; Sjöstrand, S. E.; Skånberg, I.; Sundell, G. Inhibition of Gastric Acid Secretion by Omeprazole in the Dog and Rat. *Gastroenterology* **1983**, *85* (4), 900–907.

(62) Kakooei, S.; Ismail, C.; Ari-Wahjoedi, B. An Overview of PH Sensors Based on Iridium Oxide: Fabrication and Application. *Int. J. Mater. Sci. Innov.* **2013**, *1* (1), 62–72.

(63) Klinkenberg, G.; Lystad, K. Q.; Levine, D. W.; Dyrset, N. PH-Controlled Cell Release and Biomass Distribution of Alginate-Immobilized Lactococcus Lactis Subsp. Lactis. *J. Appl. Microbiol.* **2001**, *91*, 705–714.

(64) Wilson, N. R.; Clewes, S. L.; Newton, M. E.; Unwin, P. R.; Macpherson, J. V. Impact of Grain-Dependent Boron Uptake on the Electrochemical and Electrical Properties of Polycrystalline Boron Doped Diamond Electrodes. *J. Phys. Chem. B* **2006**, *110* (11), 5639–5646.

(65) Cobb, S. J.; Macpherson, J. V. Enhancing Square Wave Voltammetry Measurements via Electrochemical Analysis of the Non-Faradaic Potential Window. *Anal. Chem.* **2019**, *91* (12), 7935–7942.

TOC

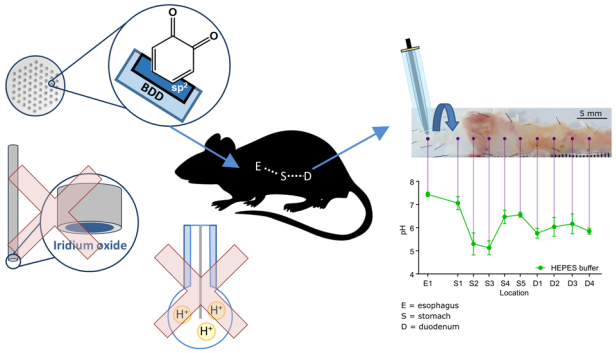
BDD
sp³
E ···· S···· D
Iridium oxide
H⁺
H⁺
H⁺
5 mm
pH
8
7
6
5
4
HEPES buffer
E1 S1 S2 S3 S4 S5 D1 D2 D3 D4
Location
E = esophagus
S = stomach
D = duodenum